Fiber Structure Formation in Ultra-High-Speed Melt Spinning of Poly(ethylene 2,6-naphthalene dicarboxylate)

KEN MIYATA, TAKESHI KIKUTANI, NORIMASA OKUI

Department of Organic and Polymeric Materials, Tokyo Institute of Technology, 2-12-1, Ookayama, Meguroku, Tokyo 152, Japan

Received 7 October 1996; accepted 29 January 1997

ABSTRACT: The high-speed melt spinning of poly(ethylene 2,6-naphthalene dicarboxylate) (PEN) was performed up to the take-up velocity of the ultra-high-speed region, 9 km/min. From the investigations of the structure and physical properties of the as-spun fibers, the high-speed spinning of PEN was divided into three regions in terms of the mechanism of fiber structure formation. The first region is the take-up velocity of up to 2.5 km/min and the birefringence of up to 0.08 where only a slight increase in molecular orientation was attained. At the take-up velocity of 2.5–4.5 km/min and the birefringence of 0.08–0.25, although some experimental evidences indicated that the orientation-induced crystallization did not occur, there was an increase in the fiber density which suggested the formation of some ordered structure. At the take-up velocity $>$ 4.5 km/min and birefringence $>$ 0.25, the orientation-induced crystallization occurred. The fibers obtained in this region were characterized by the formation of the crystalline structure dominated by the β form. The presence of the necklike deformation in the spinning line was also confirmed. The solidification temperature of the spinning line analyzed from the diameter profile suggested that the formation of β modification crystals occurred at relatively low crystallization temperatures in comparison with that in an isotropic state. Therefore it was indicated that the presence of elongational stress in the spinning line promoted the formation of the β modification crystals. © 1997 John Wiley & Sons, Inc. J Appl Polym Sci **65:** 1415–1427, 1997

Key words: high-speed melt spinning; poly(ethylene 2,6-naphthalene dicarboxylate); β modification crystals; orientation-induced crystallization; solidification temperature

INTRODUCTION

The chemical structure of poly(ethylene 2,6-naphthalene dicarboxylate) (PEN) can be described by replacing the benzene ring in poly(ethylene terephthalate) (PET) by the naphthalene ring. Accordingly, with its molecular chain stiffer than PET, PEN is expected to be one of the high-performance polymers which have high strength, high modulus, and good heat-resistance.

In contrast to PET, which crystallizes into only one crystal modification, PEN was reported to have two different crystal modifications, i.e., α and β form crystals. The α modification crystal is triclinic. The unit cell parameters are a, 0.651 nm; b, 0.575 nm; c, 1.32 nm; α, 81.33°; β, 144°; and γ, 100°.[1] The unit cell of the β form crystal was also reported to be triclinic with significantly different unit cell parameters; a, 0.926 nm; b, 1.559 nm; c, 1.273 nm; α, 121.6°; β, 95.57°; and γ, 122.52°.[2] The crystal density of the α and β modifications are 1.407 and 1.439 g/cm^3, respectively. In comparison with the α modification crystal, the characteristics of the β modification crystal may be represented by higher crystal density

Correspondence to: T. Kikutani.

 CCC 0021-8995/97/071415-13

and shorter c-axis length. In other words, the molecules in the β modification crystals are densely packed but are not fully extended along the chain direction.

Although there was a publication on the atomic coordinates of the PEN molecule in the α modification unit cell,[1] those in the β modification unit cell have not been reported yet. Buchner et al. have suggested that, compared to the chain conformation in the α form, every naphthalene ring is twisted 180° in the β form. It was also reported that the formation of the β modification crystals from the isotropic melt occurred only when the crystallization temperature was set at relatively high temperatures, i.e., 220 or 245°C.[2,3]

There already are some publications on the structure and physical properties of high-speed spun PEN fibers. Hamana et al. reported in their patent that the structure of high-speed spun PEN fibers obtained at take-up velocities of 3–7 km/min primarily consisted of β modification crystals.[4] Huijts et al. prepared high-speed spun PEN fibers and investigated the properties from the view point of industrial applications,[5] analyzed the mechanical behavior near the glass transition temperature,[6] and estimated the intrinsic birefringence.[7] Iizuka and Yabuki analyzed the relation between the necklike deformation occurring in the spinning line and the formation of fiber structure. They also estimated the ratio of the amount of α and β modification crystals in the high-speed spun PEN fibers.[8] Nagai et al. investigated the structure and properties of high-speed spun PEN fibers[9] and the change of crystal modification during the annealing of PEN fibers under stress.[10] Except for the patent by Hamana et al., the highest take-up velocities attained in these reports were limited to 5 km/min.

In the present article, the high-speed melt spinning of PEN was performed up to the take-up velocity of 9 km/min. The condition for the formation of the β modification crystals was also investigated through the on-line measurement of the thinning behavior of the spinning line.

EXPERIMENTAL

Material

Poly(ethylene 2,6-naphthalene dicarboxylate) pellet supplied by Teijin Co. Ltd. was used in this study. The intrinsic viscosity of the polymer was 0.62 dL/g. Prior to the melt spinning, the polymer was dried and crystallized through two stages. In the first stage, the polymer was held at 130°C for 8 h under vacuum. In the following stage, the temperature was raised to 210°C and kept for 2 h for the crystallization of the polymer. The crystallized polymer was preserved at 160°C under vacuum.

Melt-Spinning Process

An extrusion system consisting of an extruder and a gear pump was used for the precise control of the throughput rate. The PEN polymer was extruded from a single-hole spinneret of 1 mm diameter at 320°C. The through-put rate was controlled to 5.0 g/min. In this study, the quenching air was not applied to the spinning line. The polymer extruded from the spinneret was taken up by a high-speed winder placed at 330 cm below the spinning head. The attained highest take-up velocity was 9 km/min. The diameter of as-spun filament decreased with an increase in the take-up velocity since the throughput rate was kept constant for all the take-up velocities. The intrinsic viscosity measured for the resultant fibers was 0.48 dL/g. There was a relatively large reduction of the molecular weight during the spinning experiment. The level of molecular weight of the extruded polymer might be one of the important factors for the good spinnability attained in this work.

On-Line Measurement

A noncontact back-illumination type diameter monitor (Zimmer OHG, Model A/10) was employed for the measurement of the thinning behavior in the high-speed spinning process. The diameter was measured along the spinning line at an interval of 10 cm. The diameter data were acquired using a personal computer equipped with an A/D converter. The sampling rate and time were 2 kHz and 5 s, respectively. The diameter versus frequency diagram was prepared from the data obtained at each position to estimate the average diameter.

Birefringence

Refractive indices of the fibers parallel and perpendicular to the fiber axis were measured using an interference microscope (Carl-Zeiss Jena) equipped with a polarizing filter. Since the refractive index of PEN fiber in the direction parallel to the fiber axis was extremely high, a mixture

of methylene iodide, sulfur, and phosphorus was used as the immersion liquid. Birefringence was calculated from the two refractive indices using the following equation:

$$\Delta n = n_{\parallel} - n_{\perp} \quad (1)$$

where $n_{\parallel}$ and $n_{\perp}$ are the refractive indices parallel and perpendicular to the fiber axis, respectively.

Density

Density of the as-spun PEN fibers was measured at 25°C using a density gradient column. The liquids used for the construction of the column were *n*-heptan and carbon tetrachloride.

Wide Angle X-ray Diffraction

Wide angle X-ray diffraction (WAXD) analyses of the PEN fibers were performed using a nickel-filtered CuKα radiation source (Rigaku-Denki) generated at 40 kV–20 mA. The WAXD photographs of the fiber bundle were taken with a camera length of 4 cm. The intensity distribution curves on the equator were also measured using a goniometer.

Differential Scanning Calorimetry

The thermal analysis of the PEN fibers was performed using a differential scanning calorimeter (DSC) (Shimadzu DSC-50). In the measurement, $\sim$ 5 mg of the fiber sample which was cut to small pieces was measured at a heating rate of 20°C/min and in the temperature range of up to 320°C. From the obtained DSC thermograms, the glass transition temperature (T_g), the cold crystallization peak temperature (T_c), and the melting peak temperature (T_m) were analyzed.

Tensile Test

The load-elongation curves of the fiber samples were obtained using a tensile testing machine (Toyosokki, UTM-4L). The gauge length was 20 mm and the tensile speed was 20 mm/min. The initial Young's modulus, elongation at break, and tenacity were obtained averaging at least 10 trials of the tensile test for each sample.

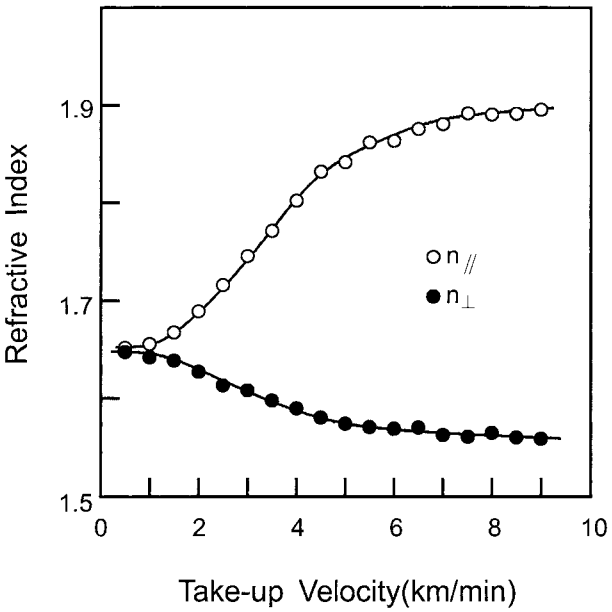

Figure 1 Refractive indices parallel and perpendicular to the fiber axis versus take-up velocity for as-spun PEN filaments.

RESULTS AND DISCUSSION

Structure and Properties of PEN Fibers

Birefringence and Density

Refractive indices parallel and perpendicular to the fiber axis, $n_{\parallel}$ and $n_{\perp}$, measured using an interference microscope, were plotted against the take-up velocity in Figure 1. With an increase in the take-up velocity, $n_{\parallel}$ increased whereas $n_{\perp}$ decreased as in the case of high-speed spun PET fibers.[11] From the result of the 0.5 km/min fiber which was essentially isotropic, the mean refractive index of PEN turned out to be $\sim$ 1.65. This value is much higher than the mean refractive index of PET, 1.575. At the take-up velocity of 9 km/min, the refractive index parallel to the fiber axis reached as high as 1.9. This is an exceptionally high value and only limited kinds of polymers such as poly(*p*-phenylene terephthalamide)[12] and poly(phenylene sulfide)[13] were reported to exhibit similar or higher values.

Birefringence of the PEN fibers was calculated as the difference between two refractive indices and plotted against the take-up velocity in Figure 2. With an increase in the take-up velocity, the birefringence showed sigmoidal increase, tended to saturate above 4.5 km/min, and reached to the highest value of 336×10^{-3} at 9 km/min. The

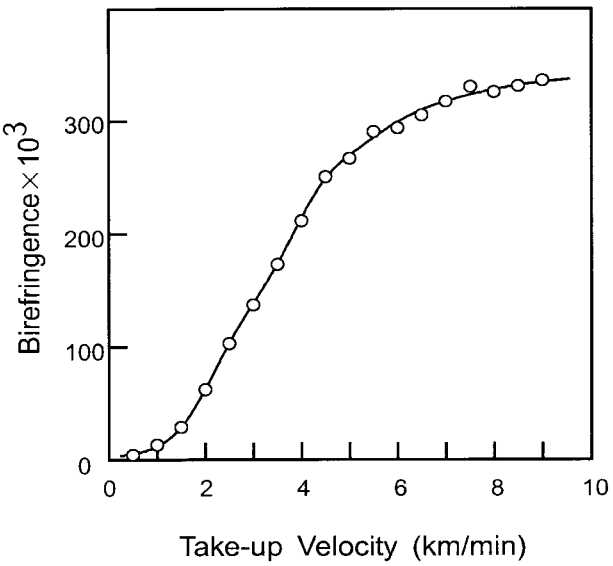

Figure 2 Effect of take-up velocity on birefringence of PEN fibers.

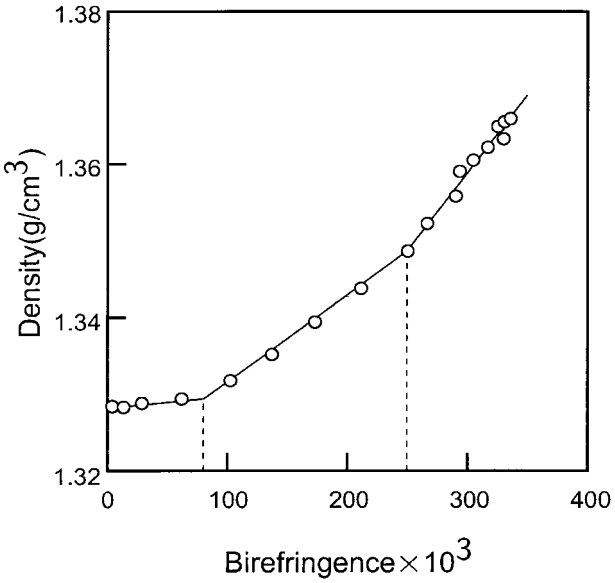

Figure 4 The relationship between birefringence and density of as-spun PEN fibers.

increase in the birefringence implies the development of molecular orientation. From the considerably high value of birefringence, it was also speculated that PEN has significantly larger intrinsic birefringence than PET.

Dependence of the density of as-spun fibers on the take-up velocity is shown in Figure 3. The density was virtually constant at low speeds, started to increase at $\sim$ 2.5 km/min, and eventually showed a tendency of saturation $> \sim$ 4.5 km/min. In comparison with the result for birefringence, the tendency of saturation was more or less moderate.

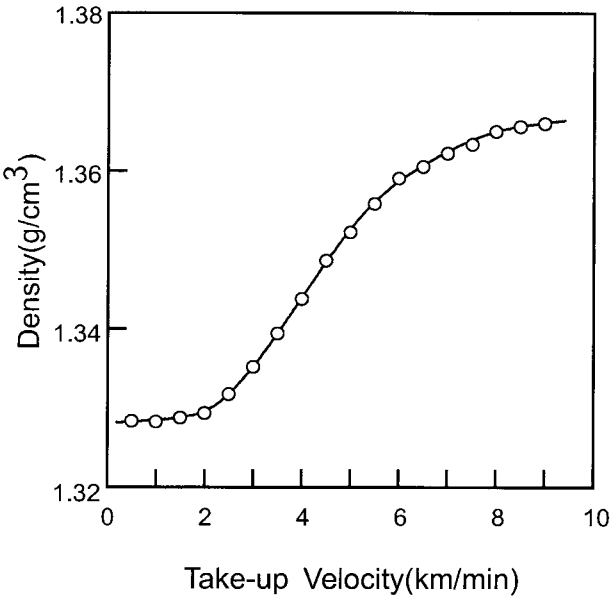

Figure 3 Effect of take-up velocity on density of PEN fibers.

The relation between birefringence and density of the as-spun filaments is shown in Figure 4. It appears that this relation can be divided into three regions. When the birefringence was <0.08, which corresponded to the take-up velocity of 2.5 km/min, the density was virtually constant. The density started to increase when the birefringence exceeded 0.08. When the birefringence became >0.25, which corresponded to the take-up velocity of 4.5 km/min where the changes of birefringence and density with the take-up velocity showed the tendency of saturation, the density increased more steeply against the birefringence. From this observation, it was speculated that the mechanism of fiber structure formation during the high-speed spinning process changed at these two break points.

In the relation between birefringence and density of the high-speed spun PET fibers, only one break point was found at the birefringence of $\sim$ 0.06, and this point was regarded as the onset point of the orientation-induced crystallization.[11] On the other hand, Iizuka and Yabuki reported that the density of high-speed spun PEN fibers started to increase remarkably at the birefringence of $\sim$ 0.17.[8] They also designated this point as the starting of the orientation-induced crystallization. Since the fibers spun at low speeds were

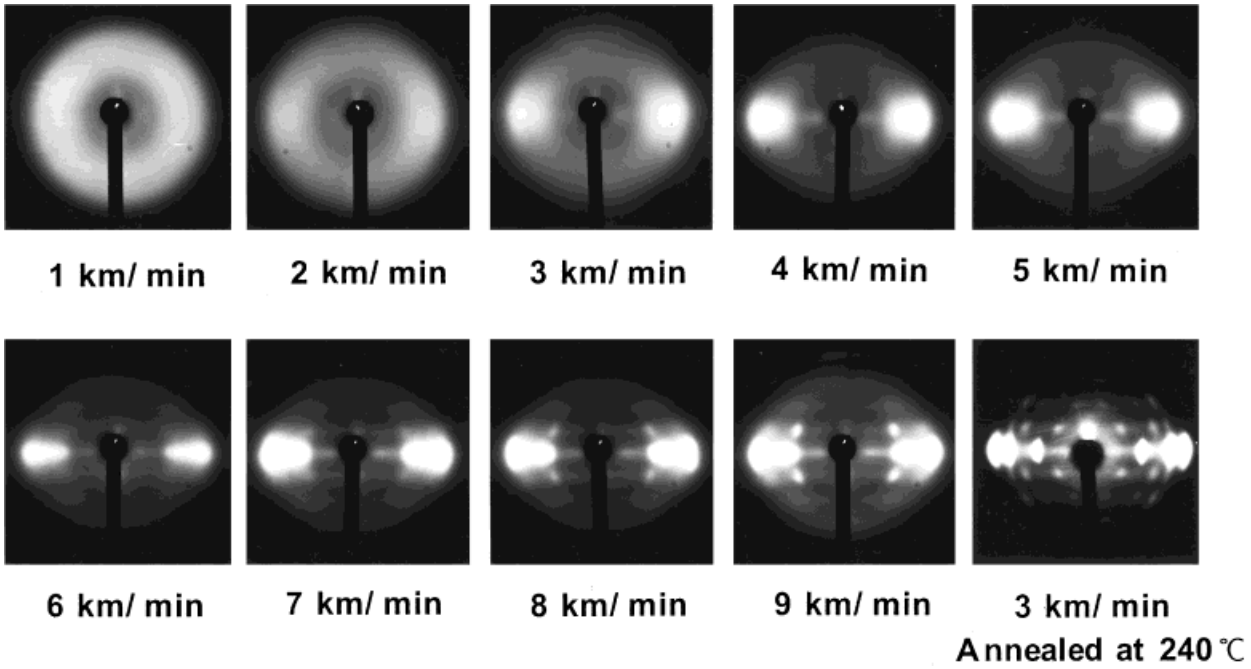

Figure 5 Wide angle X-ray diffraction patterns of as-spun fibers and the fiber prepared by annealing the as-spun 3 km/min fiber at 240°C for 1 h at a fixed length.

not studied intently in their work, the break point at the birefringence of 0.17 may correspond to our second break point at 0.25. If the differences in the spinning conditions are considered, the molecular weight of PEN fibers obtained in this work might be lower than that of their fibers. Also, the throughput rate adopted in this work was about three times larger than theirs. These two differences might have an effect to shift the structure formation behavior to the higher take-up velocities because relatively low stress in the upper region of the spinning line can be expected in our experiments.[14] Nevertheless, the reason for the difference in the relation between two structural parameters, birefringence and density, is not clear at present.

WAXD Patterns and DSC Thermograms

The WAXD patterns of the high-speed spun PEN fibers obtained at various take-up velocities are shown in Figure 5. Included in the figure for comparison is the WAXD pattern of the fiber prepared by annealing the as-spun 3 km/min fiber at 240°C for 1 h at a fixed length. In the case of as-spun fibers, only the amorphous halo was observed up to the take-up velocity of 4 km/min. The amorphous halo tended to concentrate on the equator with increasing take-up velocity indicating the development of molecular orientation. The crystalline reflections started to appear at $\sim$ 5 km/min and became fairly distinct at 8 and 9 km/min. These fibers exhibited the WAXD patterns of highly oriented β modification crystals of PEN. On the other hand, the formation of α modification crystals was confirmed in the annealed fibers.

The WAXD intensity diagrams of the PEN fibers measured on the equator are compared in Figure 6. Above 5 km/min, the reflections from (020) and (200) planes of the β modification crystals were clearly observed at $\sim 2\theta = 18.6°$ and 26.6°, respectively. These peaks became stronger and narrower with an increase in the take-up velocity, indicating the development of large and ordered crystallites. On the other hand, the co-existence of α modification crystals was also confirmed from the small shoulders at $2\theta = 15.6°$ and 23.3°. These peaks correspond to (010) and (100) reflections of α modification crystals. By comparing the diffraction intensities from the α and β modification crystals, it was recognized that the amount of α crystals relative to that of β crystals decreased with an increase in the take-up velocity.

The DSC thermograms of the high-speed spun PEN fibers are shown in Figure 7. The glass transition was clearly observed at $\sim$ 120°C for the

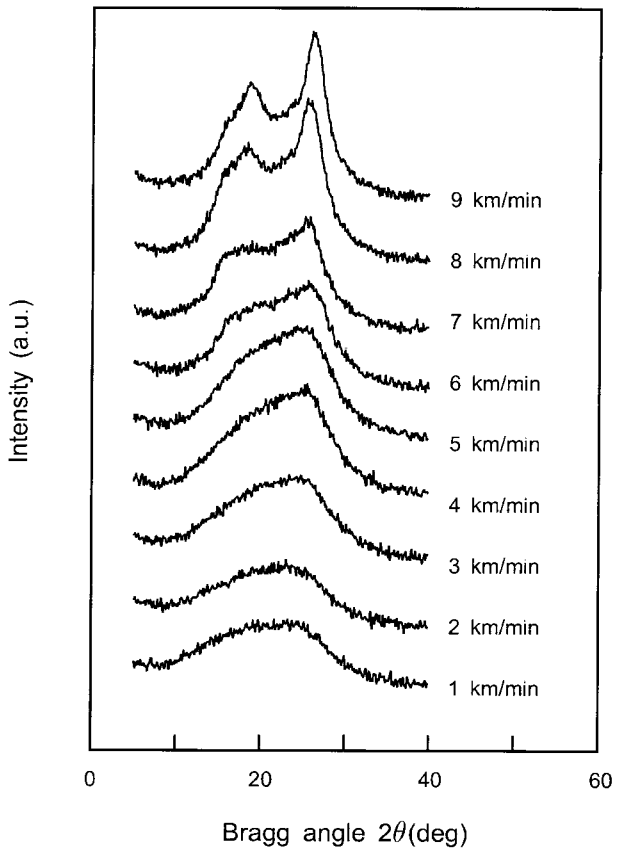

Figure 6 Wide angle X-ray diffraction intensity diagrams of as-spun PEN fibers measured on the equator.

low-speed samples; however, it became obscure at high speeds. At low speeds, an exothermic peak of cold crystallization was also observed at ~ 150–200°C. The peak shifted to lower temperatures and became smaller with increasing take-up velocity. It finally disappeared when the take-up velocity exceeded 4 km/min. On the other hand, an endothermic peak of melting, which appeared at ~ 272°C in low-speed fibers, gradually shifted to higher temperatures > 4 km/min.

The peak temperatures of cold crystallization and melting were plotted against the take-up velocity in Figure 8. The crystallization rate of amorphous fibers increases with the development of molecular orientation. Accordingly, if the temperature of the fibers is increased at a constant heating rate, the cold crystallization of the fibers with higher molecular orientation occurs at lower temperatures, as observed in the DSC diagrams. The cold crystallization peak was not detected for the fibers obtained >4 km/min, which showed crystalline reflections in the WAXD diagrams. The melting temperature also started to increase at ~ 4 km/min, and reached to 293°C at 9 km/min. The increment of melting temperature from 3 to 9 km/min was as high as 20°C.

As described above, the take-up velocity at which melting temperature of PEN fibers started to increase corresponded to the velocity at which the cold crystallization peak disappeared. A similar tendency of the relation between cold crystallization and melting was reported for the high-speed spun PET fibers,[11] and the velocity at which the thermal behavior changed was attributed to the starting point of the orientation-induced crystallization. Therefore, the results of WAXD and DSC analyses supported the consideration that the orientation-induced crystallization of the PEN fibers in the high-speed spinning process started to occur at the take-up velocity of 4–5 km/min, where the fiber birefringence of ~ 0.25 was attained.

In the case of PET, the higher melting temperature of the fibers obtained at high speeds was attributed to the formation of highly ordered large crystallites in the spinning line. The distinct crystalline reflections in the WAXD patterns of PEN fibers obtained at high speeds also indicated the

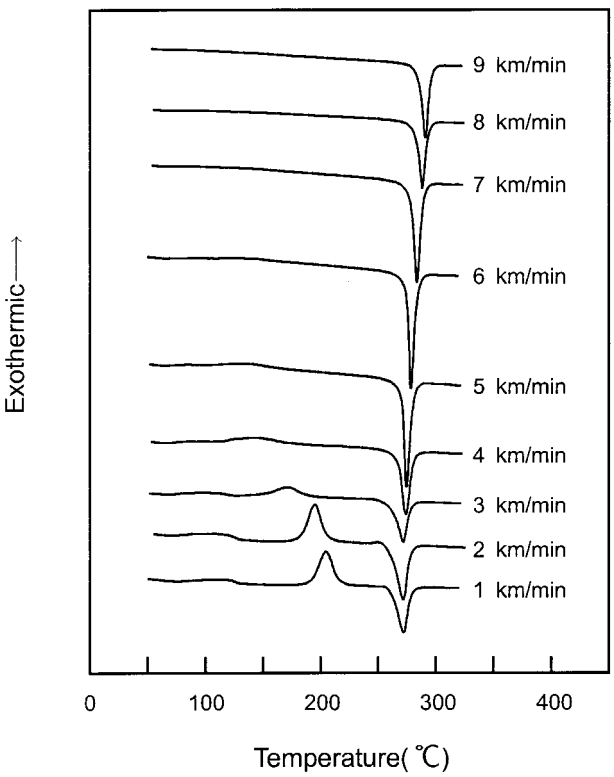

Figure 7 Differential scanning calorimeter thermograms of as-spun PEN fibers.

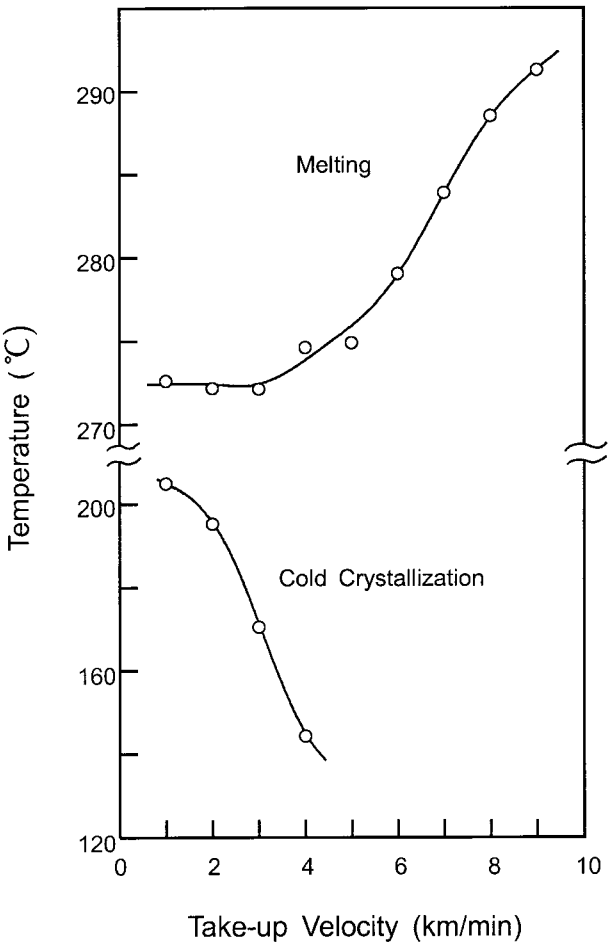

Figure 8 Peak temperatures of cold crystallization and melting plotted against the take-up velocity.

similar mechanism for the drastic increase of the melting peak temperature.

On the other hand, the formation of β modification crystals might also have some influence on the increase in melting peak temperature. It is worth noting that only one melting peak was observed in the DSC thermograms in spite of the co-existence of the α and β modification crystals, which was confirmed in the WAXD measurement. Nagai et al.[9] found a shoulder in the melting peak of high-speed spun PEN fibers and considered that the melting endotherm at lower temperature corresponds to the α form crystals. On the other hand, Buchner, Wiswe, and Zachmann investigated the melting behavior of isotropic PEN films containing the α and β crystals and discussed that the melting temperature of both the α and β crystals depends strongly on the annealing conditions and the resultant crystalline morphology.[2] Investigations on the relation between the melting behavior and the change of the structural parameters of α and β individual crystals might be necessary to clarify the melting behavior of the PEN crystals.

Spinning Dynamics and Condition for Formation of β Modification Crystals

Diameter Profiles

On-line measurement of the filament diameter in the high-speed spinning line of PEN was performed. The change of diameter versus frequency diagram with the distance from the spinneret for various take-up velocities is shown in Figure 9. At low speeds, the filament diameter attenuated smoothly in the spinning line. On the other hand, at the take-up velocities > 5 km/min, the diameter of the spinning line decreased abruptly at the end part of deformation. Because of the fluctuation of the position of the abrupt thinning, the frequency versus diameter diagrams in this region showed bimodal diameter distribution. This type of deformation, which usually is called as the

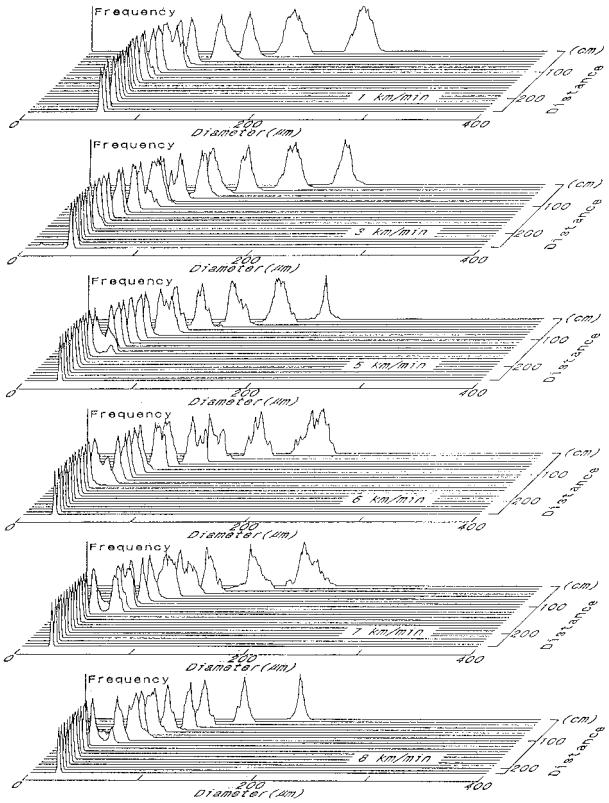

Figure 9 Change of diameter versus frequency diagram with the distance from the spinneret for various take-up velocities.

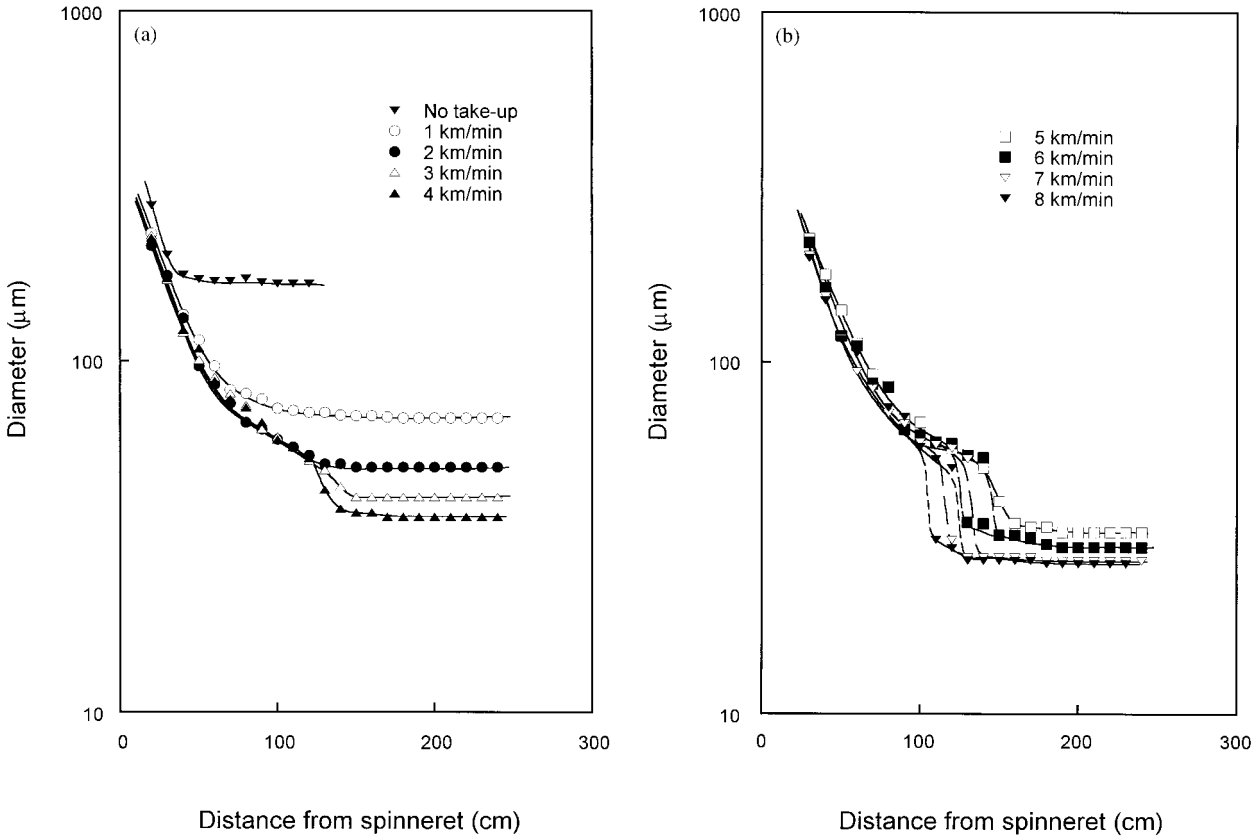

Figure 10 Diameter profiles of the spinning line of PEN obtained at various take-up velocities. (a) up to 4 km/min; (b) >4 km/min.

necklike deformation, was reported for the high-speed spinning line of various crystalline polymers.[15]

The diameter profiles of the spinning line of PEN obtained at various take-up velocities are summarized in Figure 10(a,b). At 1 km/min, an ordinary smooth-diameter profile was observed. At 3 km/min, although the deformation progressed smoothly, there was a concentration of deformation at the end part of thinning. The necklike deformation was clearly observed above 5 km/min and the position of the necklike deformation shifted toward the spinneret with an increase in the take-up velocity. At high speeds, an additional slight thinning was also observed $> \sim 20$ cm of the spinning line immediately below the steep diameter attenuation.[16]

Estimation of Filament Temperature

The change of filament temperature during the spinning process was estimated by substituting the diameter profiles shown in Figure 10 to the energy balance equation of the spinning line.

$$\frac{dT}{dx} = -\frac{\pi D h}{W C_p}(T - T_a) \tag{2}$$

where T, D, and x are the temperature, the diameter, and the distance from the spinneret, respectively; W and T_a are the throughput rate and the cooling air temperature. For the temperature dependence of the specific heat, C_p, of PEN, the equation proposed by Cheng and Wunderlich was used.[17]

$$C_p = 0.40941T + 268.35 \text{ J K}^{-1} \text{ mol}^{-1} \tag{3}$$

The convective coefficient of heat transfer h was calculated using the following equations:

$$h = \frac{k^*}{D} Nu \tag{4}$$

$$Nu = 0.28 Re^{0.32} \tag{5}$$

$$Re = \frac{DV}{\nu^*} \tag{6}$$

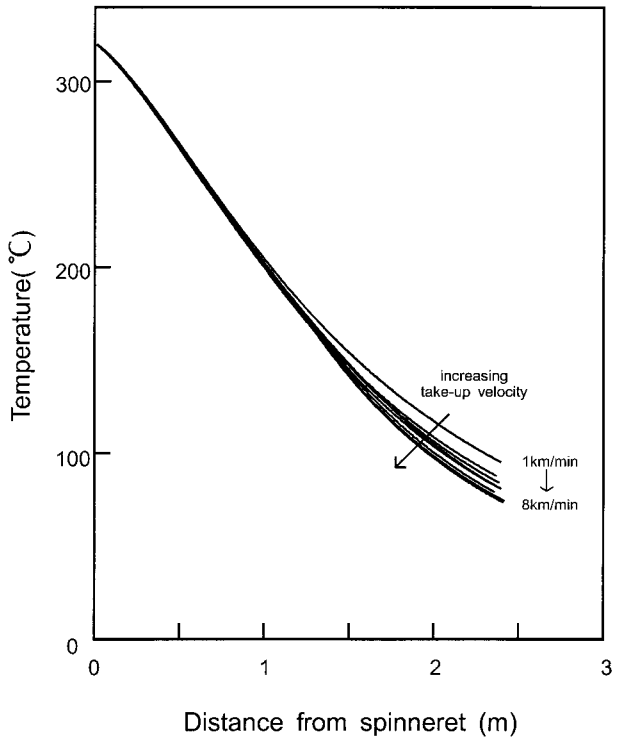

Figure 11 Temperature profiles of the spinning line calculated substituting the diameter profiles to the energy balance equation of the spinning line.

where V is the velocity of the spinning line, k^* is the heat conductivity of the air, and Nu and Re are the Nusselt number and the Reynolds number, respectively.[18] The equation (5) is an empirical equation obtained by the on-line temperature measurement of the high-speed spinning line using an infra-red radiation gauge.[19] This equation estimates slightly slower cooling of the spinning line in comparison with the frequently used empirical equation proposed by Kase and Matsuo[18]:

$$Nu = 0.42Re^{0.33} \tag{7}$$

The following constants were used for k^* and the kinematic viscosity of the air, ν^*:

$$k^* = 2.60 \times 10^{-2}\ \mathrm{W\ m^{-1}\ K^{-1}}\ (25°\mathrm{C});$$

$$\nu^* = 18.2 \times 10^{-6}\ \mathrm{Pa\ s}\ (25°\mathrm{C})$$

The temperature profiles of the spinning line calculated using the above equations are shown in Figure 11. Temperature profiles slightly shifted toward lower temperatures with increasing take-up velocity.

Solidification Temperature and Structure Formation

By comparing Figures 10 and 11, the solidification temperatures of the spinning line were estimated and plotted against the take-up velocity as shown in Figure 12. When the take-up velocity was low and the as-spun filaments had amorphous structure, the solidification of the spinning line was expected to occur at the glass transition temperature of PEN. It can be seen from Figure 12 that the estimated solidification temperature up to the take-up velocity of 4 km/min was virtually constant at $\sim$ 125°C. This temperature agreed well with the glass transition temperature observed in the DSC diagrams shown in Figure 7. The small difference between the analyzed solidification and glass transition temperatures suggested that there was a slight overestimation of the temperature of the spinning line in this calculation. When the take-up velocity was $>$ 4 km/min, the solidification temperature increased with an increase in the take-up velocity. The estimated solidification temperature for 8 km/min was $\sim$ 180°C.

It is important to point out that the major part of crystallization in the spinning line is considered to occur near or below the solidification position. This implies that the orientation-induced crystallization to form the β modification crystals occurred below 180°C in the spinning line. On the other hand, it was reported that the β modifica-

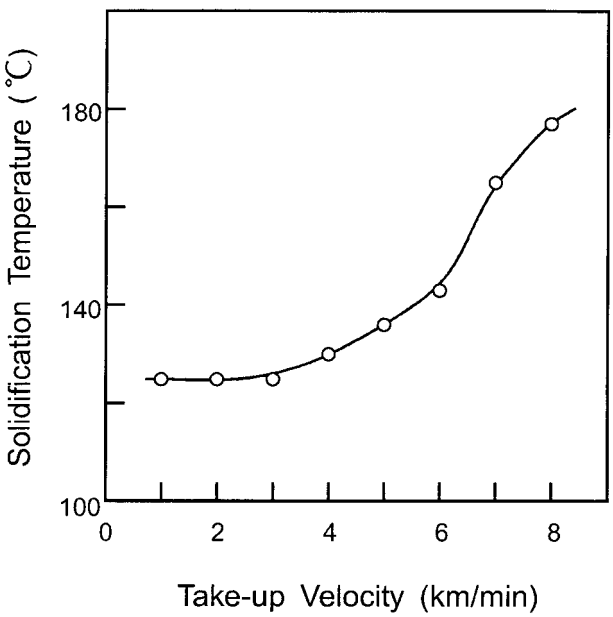

Figure 12 Estimated solidification temperatures of the spinning line plotted against the take-up velocity.

tion crystals can be formed only at very high temperatures, i.e., $> 220°C$[2] or $245°C$[3] in an isotropic state. Therefore, it was suggested that the elongational stress applied to the fiber in the spinning line had an effect to promote the formation of β modification crystals at relatively low temperatures. It is interesting to realize that the c-axis length of the unit cell of the β modification crystals is shorter than that of the α modification crystals. On the other hand, the crystal density of the β form is larger than that of the α form. Therefore, it appears that even under the circumstance of uniaxial elongational stress field, the formation of crystals, in which molecular chains are densely packed in lateral direction, was more preferable than the ones in which molecular chains are fully extended.

Even though there were many reports on the crystalline structure development of various polymers in the high-speed melt spinning process, most of those fibers exhibited only one crystal modification. One exception is the case for polyamide 6. Shimizu et al.[20] reported that in the high-speed melt spinning of polyamide 6, the amount of the sum of γ and pseudohexagonal modification crystals increased, while that of the α modification crystals decreased with an increase in the take-up velocity. In this case, the γ modification crystals had shorter c-axis length and lower crystal density than the α modification crystals. Because the hydrogen-bond sheets in the γ crystals are formed by the parallel chains and those in the α crystals are formed by the anti-parallel chains, it was considered that the preference of the formation of intra or intermolecular hydrogen bonds in the course of crystallization made this difference. In case of PEN, there might be a significant mutual interaction between the naphthalene rings in adjacent molecules. Therefore, we are considering that the stacking of naphthalene rings between molecules oriented and aligned parallel to each other had a certain effect on the formation of β modification crystals.

In contrast to the preferred formation of the β modification crystals from the melt under uniaxial stress, it was reported that the stress applied in the drawing and annealing processes brings about the formation of the α modification crystals. Murakami et al.[21] reported that only α modification crystal was formed and the β modification crystal was not observed in the uniaxial drawing of amorphous PEN films. Nagai et al.[10] reported that the crystal transition from the β form to the α form occurred when high elongational stress was applied to the high-speed spun PEN filaments, even below the glass transition temperature, i.e., 50–100°C.

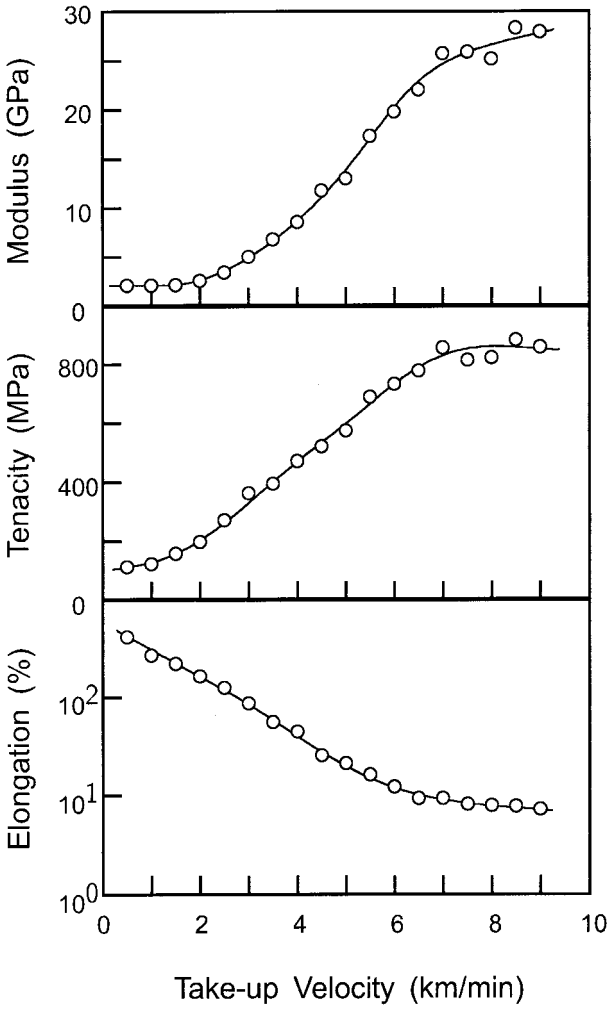

Figure 13 The initial Young's modulus, tenacity, and elongation at break of the PEN fibers plotted against the take-up velocity.

Mechanical Properties

The initial Young's modulus, tenacity, and elongation at break of the PEN fibers are plotted against the take-up velocity in Figure 13. The modulus and the tenacity increased, and the elongation decreased with an increase in the take-up velocity. The modulus of 28 GPa and the tenacity of 800 MPa were obtained at 9 km/min. It was reported that the high-speed spun PET fibers have the modulus of $\sim$ 10 GPa and the tenacity of $\sim$ 500 MPa.[22] The mechanical properties of high-speed spun PEN fibers were significantly higher than

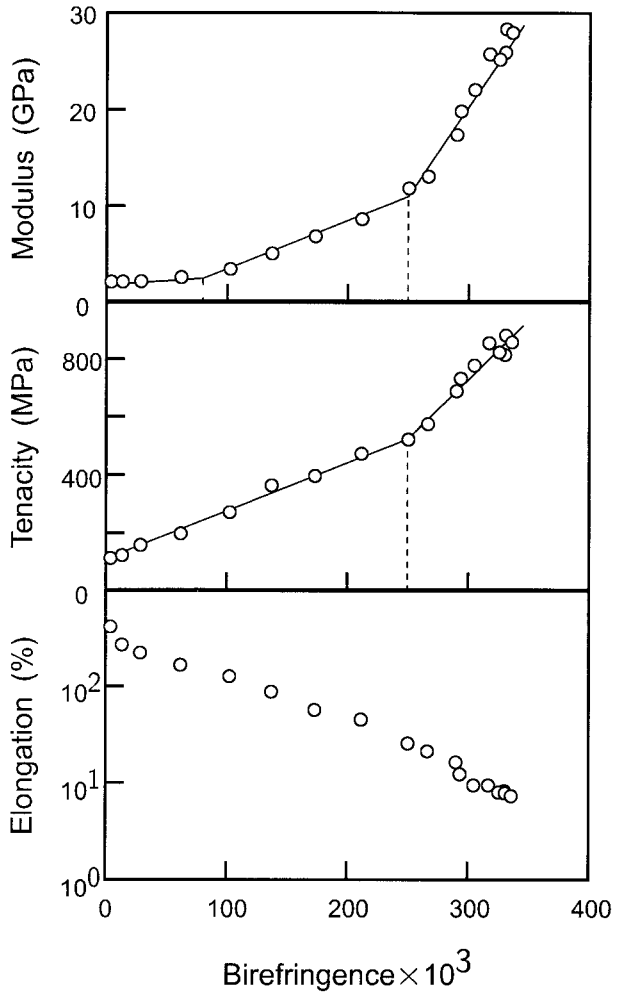

Figure 14 The initial Young's modulus, tenacity, and elongation at break of the PEN fibers plotted against birefringence.

those of PET fibers, presumably owing to the higher rigidity of the molecular chain. On the other hand, Ito, Honda, and Kanamoto[23] reported the modulus of 29 GPa and the tenacity of 1.1 GPa for the PEN fibers prepared by a two-stage drawing process. Therefore, it can be said that the mechanical properties of the high-speed spun PEN fibers are comparable to the PEN fibers prepared through intensive drawing and annealing processes.

The mechanical properties of the PEN fibers were plotted against birefringence in Figure 14. The initial Young's modulus showed a break point at the birefringence of ~ 0.08 where a similar break point was observed in the density versus birefringence plot. Even though there is no indication of the formation of crystals, it appears that there is a starting of the formation of some ordered structure at this point. Both the modulus and tenacity showed steep increases when the birefringence exceeded 0.25 where the orientation-induced crystallization started. The crystalline modulus for α modification crystals was reported as 145 GPa by Nakamae, Nishino, and Gotoh.[24] On the contrary, the crystalline modulus for the β modification crystals has not been reported yet. Therefore it is not clear at present whether the formation of β modification crystals is more advantageous than the α crystals in terms of the improvement of mechanical properties.

Molar Polarizability

The molar polarizability is an important parameter for the characterization of the structure of polymers. The parameter can be used for the theoretical estimation of the refractive indices and the intrinsic birefringences. From the experimental aspects, it can be used for the analysis of density distribution in the cross section of fibers employing the data on the distribution of refractive indices.[13] It can also be used for the estimation of the composition of copolymers from the relation between mean refractive index and the density of fibers.[25] Because parameters related to the polarizability of the naphthalene ring have not been reported yet, the polarizability of the repeating unit of PEN was estimated.

The Lorentz–Lorenz equation expresses the relation between refractive index n and density ρ of the filament as follows.

$$\frac{n^2 - 1}{n^2 + 2} = \frac{4\pi N\rho}{3M} P \tag{8}$$

where N, M, and P denote the Avogadro number, the molecular weight, and the molar polarizability, respectively. For a uniaxially anisotropic material such as filaments, the mean refractive index n may be expressed using the refractive indices parallel and perpendicular to the principal axis ($n_\parallel$, $n_\perp$) as follows.

$$n^2 = \frac{2n_\perp^2 + n_\parallel^2}{3} \tag{9}$$

According to eqs. (8) and (9), the value $(n^2 - 1)/(n^2 + 2)$ calculated using the experimental data

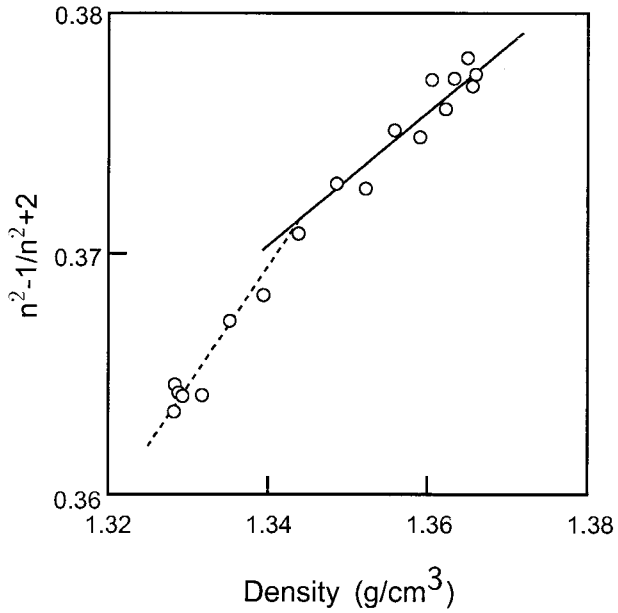

Figure 15 Plots of $(n^2 - 1)/(n^2 + 2)$ against density. The mean refractive index n was calculated from the experimental data shown in Figure 1.

in Figure 1 were plotted against the density as shown in Figure 15.

A break point was observed at the density of 1.344 g/cm^3, which corresponded to the take-up velocity of 4 km/min and also to the onset point of the orientation-induced crystallization. For the data with density higher than this break point, a straight line which passes through the origin was fitted by the least-square method. The specific refractivity $(4\pi N\rho/3M)$ and polarizability of PEN calculated from the slope were 0.2759 cm^3/g and 2.648×10^{-23} cm^3, respectively. On the other hand, the molar polarizability of PEN was calculated assuming the additivity of the bond polarizabilities. In the calculation, the bond polarizabilities proposed by Bunn was used.[26] The bond polarizabilities for the carbons in the benzene ring were used as substitutes for those in the naphthalene ring. The obtained specific refractivity and molar polarizability were 0.2646 cm^3/g and 2.540×10^{-23} cm^3. These values were $\sim$ 4% lower than those obtained from the experimental results, revealing that the bond polarizabilities related to the naphthalene ring are higher than those related to the benzene ring. Since the data for the crystallized samples fitted well to a straight line which passes through the origin, it was also suggested that there was an increase in the molar polarizability for the amorphous samples with an increase in the molecular orientation. This observation indicates the presence of the effect of the internal field.[27] A higher possibility of the stacking of planar naphthalene rings with the development of molecular orientation was considered to be the origin of this effect.

CONCLUSIONS

From the experimental results described above, the mechanism of fiber structure formation in the high-speed melt spinning of PEN can be divided into three regions. The first region is the take-up velocity of up to 2.5 km/min and the birefringence of up to 0.08. This region can be regarded as the ordinary low-speed spinning in which only a slight increase of molecular orientation was attained. At the take-up velocity of 2.5–4.5 km/min and the birefringence of 0.08–0.25, although there was no indication of crystallization, a certain degree of structural ordering appeared to be developed. The occurrence of the orientation-induced crystallization in this region can be dismissed by the presence of a cold crystallization peak in the DSC diagrams, the appearance of no distinct crystalline reflections in the WAXD patterns, and the solidification of the spinning line at around the glass transition temperature. On the other hand, the increase in the density and the molar polarizability, the distinct concentration of amorphous halo on the equator, and the concentration of deformation near the solidification point in the spinning line can be regarded as the evidence for the formation of some ordered structure. At the take-up velocity of $>$ 4.5 km/min and birefringence $>$ 0.25, the orientation-induced crystallization occurred. The change in crystallization behavior with an increase in the take-up velocity can be characterized by the tendency of saturation of birefringence and density, the formation of β form rich crystalline structure, the rise in the melting peak temperature, and the improvement in the mechanical properties. The necklike deformation was observed in the spinning line and the solidification temperature increased with the take-up velocity. The formation of β modification crystals occurred at relatively low crystallization temperatures presumably because of the presence of elongational stress in the spinning line.

REFERENCES

1. Z. Mencik, *Chem. Prum.,* **42,** 78 (1967).
2. S. Buchner, D. Wiswe, and H. G. Zachmann, *Polymer,* **30,** 480 (1989).

3. M. Cakmak, Y. D. Wang, and M. Simhambhatla, *Polym. Eng. Sci.,* **30,** 12, 721 (1990).
4. I. Hamana, Y. Fujiwara, and S. Kumakawa, Jpn. Pat. 5612 (1977) (to Teijin Ltd.).
5. J. Jager, J. A. Juijn, C. J. M. van den Heuvel, and R. A. Huijts, *J. Appl. Polym. Sci.,* **57,** 1429 (1995).
6. R. A. Huijts and A. J. de Vries, Intern. *J. Polym. Mater.,* **22,** 231 (1993).
7. R. A. Huijts and S. M. Peters, *Polymer,* **35,** 3119 (1994).
8. N. Iizuka and K. Yabuki, *Sen'i Gakkaishi,* **51,** 463 (1995).
9. A. Nagai, Y. Murase, T. Kuroda, M. Matsui, Y. Mitsuishi, and T. Miyamoto, *Sen'i Gakkaishi,* **51,** 470 (1995).
10. A. Nagai, Y. Murase, T. Kuroda, M. Matsui, Y. Mitsuishi, and T. Miyamoto, *Sen'i Gakkaishi,* **51,** 478 (1995).
11. J. Shimizu, N. Okui, and T. Kikutani, *Sen'i Gakkaishi,* **37,** T-135 (1981).
12. S. Manabe, S. Kajita, and K. Kamide, *Sen'i Kikai Gakkaishi,* **34,** T98 (1981).
13. T. Kikutani, K. Wakayama, M. Sato, and A. Takaku, *Sen'i Gakkaishi,* **48,** 549 (1992).
14. A. Ziabicki, *Fundamentals of Fiber Formation,* John Wiley and Sons, New York, 1976, p. 208.
15. J. Shimizu, *Sen'i Kikai Gakkaishi,* **38,** P243 (1985).
16. T. Kikutani, N. Ogawa, and N. Okui, extended abstracts of the Polymer Processing Society 12th Annual Meeting, Sorrento, Italy, 1996, p. 315.
17. S. Z. D. Cheng and B. Wunderlich, *Macromolecules,* **21,** 789 (1988).
18. S. Kase and T. Matsuo, *J. Polym. Sci., A,* **3,** 2541 (1965).
19. T. Kikutani, Y. Kawahara, T. Matsui, A. Takaku, and J. Shimizu, *Seikei-kakou,* **1,** 333 (1988).
20. J. Shimizu, N. Okui, T. Kikutani, A. Ono, and A. Takaku, *Sen-i Gakkaishi,* **37,** 143 (1981).
21. S. Murakami, Y. Nishikawa, M. Tsuji, A. Kawaguchi, S. Kohjiya, and M. Cakmak, *Polymer,* **36,** 291 (1995).
22. T. Nakajima, *Advanced Fiber Spinning Technology,* Woodhead Publishing Ltd., Cambridge, 1994.
23. M. Ito, K. Honda, and T. Kanamoto, *J. Appl. Polym. Sci.,* **46,** 1013 (1992).
24. K. Nakamae, T. Nishino, and Y. Gotoh, *Polymer,* **36,** 1401 (1995).
25. T. Kikutani, K. Morohoshi, H. Y. Yoo, S. Umemoto, and N. Okui, *Polym. Eng. Sci.,* **35,** 942 (1995).
26. C. W. Bunn, *Chemical Crystallography,* Clarendon Press, Oxford, 1961.
27. S. D. Hong, C. Chang, and R. Stein, *J. Polym. Sci.,* **13,** 1447 (1975).